ORIGINAL PAPER

Magnetic nanocomposite-based SELDI probe for extraction and detection of drugs, amino acids and fatty acids

Mohamed O. Amin[1] · Bessy D'Cruz[1] · Metwally Madkour[1] · Entesar Al-Hetlani[1]

Abstract

The use of carbon black-Fe_3O_4 magnetic nanocomposite (CB-Fe_3O_4) as a probe for surface-enhanced laser desorption ionization mass spectrometry (SELDI-MS) with a high extraction efficiency and sensitive detection is described. The magnetic nanocomposite was synthesized and fully characterized using X-ray photoelectron spectroscopy, X-ray diffraction, Raman spectroscopy, Fourier transform infrared spectroscopy, Ultraviolet-Visible spectroscopy, transmission electron microscopy and nitrogen sorption. The feasibility of the SELDI probe to extract and detect three classes of drugs (labetalol, metoprolol, doxepin, desipramine, triprolidine and methapyrilene) spiked in wine is demonstrated. All the drugs were successfully and reproducibly extracted and detected with high efficiency and with limits of detection (LOD) between 1 and 1000 pg mL^{-1}. The adsorption capacity of the nanocomposite for the drugs was evaluated by UV-Vis spectroscopy. The results showed that 27.8–36.1% of the drugs were adsorbed on the magnetic probe within 3 min. The nanocomposite was also applied for efficient analysis of amino acids and fatty acids. Both types of analytes can be extracted within a few minutes and then successfully quantified by SELDI-MS.

Keywords Surface-enhanced laser desorption ionization mass spectrometry · Magnetic probe · Small molecules · Extraction · β-Blockers · Antidepressant · Antihistamine · Biomolecules

Introduction

The escalation in the number crime reports has prompted the development of reliable, convenient and cost-effective approaches to perform analyses that can fulfill jurisdictional requirements and are scientifically supported by robust analytical techniques [1]. These analyses should be performed with high-throughput and efficient methods, especially in local and federal laboratories where evidence is subjected to multiple analyses on a regular basis. Specifically, the occurrence of drug consumption and abuse has risen rapidly in most modern societies. Therefore, there is an increasing demand for improved confirmatory techniques for the analysis and identification of controlled substances that might be present at crime scenes [2].

Surface-assisted laser desorption ionization-mass spectrometry (SALDI-MS) has emerged as a substantial technique offering rapid analysis with high discriminatory power in various fields, especially forensic science [2]. SALDI-MS utilizes active substrates, including nanoparticles (NPs), quantum dots (QDs), functionalized carbon-based materials and metal organic-frameworks (MOFs), hence avoiding common issues encountered with the conventional MALDI techniques, such as matrix interferences in the low mass region and the presence of a 'sweet spot' [3, 4]. Additionally, SALDI technique offers low sample consumption, a very high detection sensitivity and a limit of detection (LOD) in the femto-mole range, thus facilitating the analysis of trace evidence, where minute amounts of sample are available [5]. Furthermore, SALDI analysis has been used to detect drugs that can be present in latent fingerprints [6], beverage samples [7] and saliva [8].

In forensic analyses, it is sometimes imperative to extract targeted drug(s) (i.e., substances of interest) from samples. This requires the use of conventional chromatography (such as GC or HPLC) and other purification techniques, which can

✉ Mohamed O. Amin
   Mohamed.amin@ku.edu.kw

✉ Entesar Al-Hetlani
   Entesar.alhetlani@ku.edu.kw; entesaralhetlani@gmail.com

[1] Faculty of Science, Department of Chemistry, Kuwait University, P.O. Box: 5969, 13060 Kuwait City, Kuwait

be tedious and time consuming. Therefore, surface-enhanced laser desorption ionization mass-spectrometry (SELDI-MS) has advanced since 1993 and has served as a powerful complementary technique to SALDI [9]. SELDI technique eliminates the use of conventional organic matrices and utilizes an active probe for direct extraction, purification, enrichment, desorption and ionization of the targeted analyte, thereby reducing the time required for sample pretreatment. Furthermore, a SELDI probe can be manipulated and functionalized to enhance its specificity and selectivity for different applications [10].

Many studies have employed nanomaterials as efficient adsorbents for the enrichment of analytes; for example, zeolite nanocrystals have been used to enrich peptides and proteins [11] and mesoporous silica particles have been used to enrich small molecules [12]. Nevertheless, these techniques require ultrahigh centrifugation, which can be laborious and may lead to the co-separation of undesirable molecules [13] and can hinder the analysis of small molecules due to the presence of organic matrices necessary for the analysis. Most SELDI probes have been used in proteomics and biological samples [14], or they have been used in medical diagnostics to identify biomarkers associated with specific lesions (e.g., lung and ovarian cancers) [15].

Thus far, there is a great demand for fast and effective tools that can be directly employed in forensic laboratories. Therefore, the main goal of this study is to construct a platform that can be used by forensic chemists to rapidly extract and subsequently analyze evidence that might be collected from a crime scene. In this work, a carbon black-Fe_3O_4 (CB-Fe_3O_4) magnetic nanocomposite was synthesized and fully characterized using various analytical methods. The feasibility of the magnetic nanocomposite to act as a SELDI probe for the detection of various drugs spiked in wine was investigated. The Fe_3O_4 NPs exhibit a strong spectral absorption in the UV region [6], enabling the high absorption efficiency of the laser irradiation and subsequent transfer of energy to the analyte(s) mainly via thermal effects. Furthermore, the Fe_3O_4 NPs possess good magnetic properties, facilitating the isolation of the analyte(s) in the solution [13]. On the other hand, the unique properties of CB, including large surface area, low thermal conductivity and various surface functionalities, endow the nanocomposite with high loading capacities for analytes with different functional groups. Thus, combining the distinctive properties of Fe_3O_4 NPs with those of CB forms a magnetic nanocomposite with remarkable physicochemical, optical and magnetic properties, which can be used to extract and detect analytes present in individual's drinks, and this is the primary aim of this study.

Experimental

Chemicals

Iron(III) chloride ($FeCl_3$, reagent grade, 97%), iron(II) chloride ($FeCl_2$, 98%), ammonium hydroxide (NH_4OH, 28–30%), serine (ReagentPlus®, ≥99% (HPLC)), valine (reagent grade, ≥98% (HPLC)), tryptophan (reagent grade, ≥98% (HPLC)), myristic acid (Sigma Grade, ≥99%), arachidic acid (≥99%), labetalol hydrochloride (powder, >98% (TLC)), metoprolol tartrate (≥98%), doxepin hydrochloride (≥98% (GC)), desipramine hydrochloride (powder, ≥98% (TLC)), triprolidine hydrochloride (≥99%) and methapyrilene hydrochloride (analytical standard) were purchased from Sigma Aldrich (www.sigmaaldrich.com). C65 conductive carbon black (CB) was obtained from MTI Corporation (www.mtixtl.com). All the chemicals were used without further purification, and double-distilled water (DI-water) was obtained from an Elix Milli Q water deionizer, which was used for all the experiments.

Synthesis of the carbon black-Fe_3O_4 magnetic nanocomposite (CB-Fe_3O_4)

The magnetic CB-Fe_3O_4 nanocomposite was synthesized by mixing 0.20 g of CB with an aqueous solution containing 6.10 g of $FeCl_3$ and 1.88 g of $FeCl_2$. Then, 10.00 mL of an NH_4OH aqueous solution (28–30%) was added dropwise to the mixture, and the resulting mixture was stirred for 60 min at room temperature. The precipitate was collected using an external magnet and washed several times with DI-water and, finally, with ethanol. The magnetic nanocomposite was dried overnight in an oven at 80 °C.

Characterization of the CB-Fe_3O_4 nanocomposite

The surface elemental analysis of the magnetic Fe_3O_4-CB nanocomposite was carried out by X-ray photoelectron spectroscopy (XPS) using an ESCALAB250 xi XPS spectrometer with an Al Kα monochromatic source and a charge neutralizer. The binding energies are referenced to the C 1s peak at 284.5 eV. The powder X-ray diffraction (XRD) patterns were obtained using a Bruker, D8 ADVANCE diffractometer with a Cu Kα radiation source (λ = 0.1542 nm) operating at 40 kV and 40 mA, and the scanning range was 10–80° 2θ. Raman spectra were obtained using a Renishaw inVia confocal Raman spectrometer connected to a CCD camera detector; an argon ion laser was used, where the excitation wavelength was 514.5 nm, the exposure time was 10 s, and the grating was 2400 1 mm^{-1}. Fourier transform infrared spectroscopy (FT-IR) was used to characterize the various functional groups present on the magnetic nanocomposites using a Jasco 6300 FT-IR instrument in the

range of 400–4000 cm^{-1}. A scanning speed of 2 mm s^{-1} was used to analyze the samples. The optical properties were investigated by collecting UV-Vis spectra on an Agilent Cary 5000 Scan UV-Vis-near-infrared (UV-Vis-NIR) spectrophotometer. The surface area analysis was performed using the Brunauer–Emmett–Teller (BET) method; this method was applied to the adsorption data by measuring the nitrogen sorption isotherms of the samples at −195 °C on a model Gemini VII, ASAP 2020 automatic Micromeritics sorptometer (USA). The samples were degassed at 110 °C for 12 h prior to the analysis. The morphologies of the magnetic nanocomposite were analyzed using transmission electron microscopy (TEM), and the TEM images of the nanocomposites were acquired using a JEOL JEM 1230 (JEOL Ltd., Japan) instrument operating at 120 kV.

Sample preparation for SELDI-TOF-MS

Solutions of β-blockers (labetalol and metoprolol), antidepressants (doxepin and desipramine), antihistamines (triprolidine and methapyrilene), amino acids (serine, valine and tryptophan) and fatty acids (myristic acid C14 and arachidic acid C20) were prepared separately in DI-water (the final concentrations were 1 mg mL^{-1}). All the drug standards were accurately weighed and diluted with DI-water to obtain concentrations from 1 mg mL^{-1} to 1 pg mL^{-1} for each class of drugs. Wine was spiked with an equal volume of the drug mixture, and the spiked wine was sonicated for 30 min to homogenize the mixture.

Both spiked and unspiked wine samples were studied using the magnetic nanocomposite-based SELDI probe. The samples were prepared for SELDI-TOF-MS analysis as follows: 1 mg of the magnetic nanocomposite was introduced into a microcentrifuge tube containing 2 mL of either spiked or unspiked wine, and then, the mixture was vortexed for 3 min. The magnetic composite was removed with the aid of an external magnet and redispersed in 1 mL of ethanol. The mixture was sonicated for 15–20 min, and then, 2 μL of the suspension was deposited on a polished steel target plate and allowed to dry at room temperature. Meanwhile, the analyses of the amino acids and fatty acids were carried out as follows: 1 mg of the magnetic nanocomposite was introduced into a microcentrifuge tube containing 1 mL of either the amino acids or the fatty acids solutions. The mixture was vortexed for 3 min, and then, the liquid was decanted using an external magnet. Thereafter, the magnetic nanocomposite was redispersed in 1 mL of ethanol and sonicated for 15–20 min. Then, 2 μL of the suspension was deposited on a polished steel target plate and allowed to dry at room temperature.

SELDI-TOF-MS analysis

Mass spectra were obtained using a Bruker ultrafleXtreme system equipped with a Smartbeam II laser using a reflectron time-of-flight mass spectrometer. The analyses of the β-blockers, antidepressants and antihistamines were performed in positive ionization mode using 20% laser power, and 500 shots, on average, were collected for each sample. On the other hand, the analyses of the amino acids and fatty acids were conducted in negative ionization mode using a reflectron time-of-flight mass spectrometer and 40% laser power, and 500 shots, on average, were collected for each sample. The average spectra were obtained for the analytes using a random walk raster with a frequency of 2000 Hz over a mass range of 100–500 Da. The instrument was calibrated prior to the analyses using a ProteoMass™ calibrant mix with a normal range, and the data processing was performed using Bruker flexAnalysis.

Reproducibility and LOD measurement

The reproducibility of the magnetic nanocomposite was determined by acquiring 5–6 spectra for each sample, and the average intensities and relative standard deviations (%RSDs) were calculated. For the LOD determination, a range of concentrations of the drugs (from 1 mg mL^{-1} to 1 pg mL^{-1}) were spiked into wine, and these spiked samples were subjected to analysis using the magnetic nanocomposite-based SELDI probe. The results of the LOD were considered as the investigated analyte produced a signal-to-noise ratio greater than 3 for the spectral peak.

Adsorption experiment

The amount of drug adsorbed on the magnetic nanocomposite was estimated as follows: 1 mL of the drug (100 μg mL^{-1}) solution was spiked into 1 mL of DI-water. The mixture was sonicated for 15 min. Then, 1 mg of the magnetic nanocomposite was introduced into the mixture, and the mixture was vortexed for 3 min. The UV-Vis spectra were obtained for the drug solutions before and after applying the magnetic nanocomposite and recorded using a UV-Vis spectrometer. The experiment was performed in triplicate, and the average adsorption efficiency (AE) and %RSD of the magnetic probe for the investigated drugs were calculated using the following equation:

$$\%\text{AE} = \frac{(C_o - C_t)}{CO} \times 100 \tag{1}$$

where Co and Ct represent the initial drug concentration and the drug concentration at time t, respectively.

The effect of time on the AE of the SELDI probe was carried out using the same experimental procedure; however, the concentration of the drugs was evaluated at definite time intervals and analyzed spectrophotometrically.

Results and discussion

Characterization of the carbon black-Fe₃O₄ magnetic nanocomposite (CB-Fe₃O₄)

XPS was used to determine the elemental composition and oxidation state of the magnetic nanocomposite. Figure 1a-c shows the XPS spectra of the CB-Fe₃O₄ nanocomposite,

which confirmed the presence of Fe, O and C. In Fig. 1a, the binding energies at 711.3 and 724.5 eV were attributed to Fe $2p_{3/2}$ and Fe $2p_{1/2}$ of iron oxide, respectively, which can be deconvoluted to six peaks at 710.5, 711.6, 713.8, 723.5, 724.9 and 727.1 eV [16]. The peaks at 710.5, 711.6, 723.5 and 724.9 eV corresponded to the Fe-O bond of the Fe^{2+} ion, whereas the peaks at 713.8 and 727.1 eV were assigned to the Fe-O bond of the Fe^{3+} ion in the Fe_3O_4 phase [17]. Furthermore, the small satellite peaks at 719.2 and 733.1 eV were attributed to Fe^{3+} in the Fe_2O_3 phase, revealing that the surface of the magnetic nanocomposites were slightly oxidized in the environment [16]. The photoemission spectra of O 1s can be deconvoluted into two peaks at 530.5 and 531.8 eV, which can be assigned to Fe-O and H-O, as shown in Fig. 1b [18]. Furthermore, the XPS spectrum of C 1s, as shown in Fig. 1c, was deconvoluted into three peaks at 284.7,
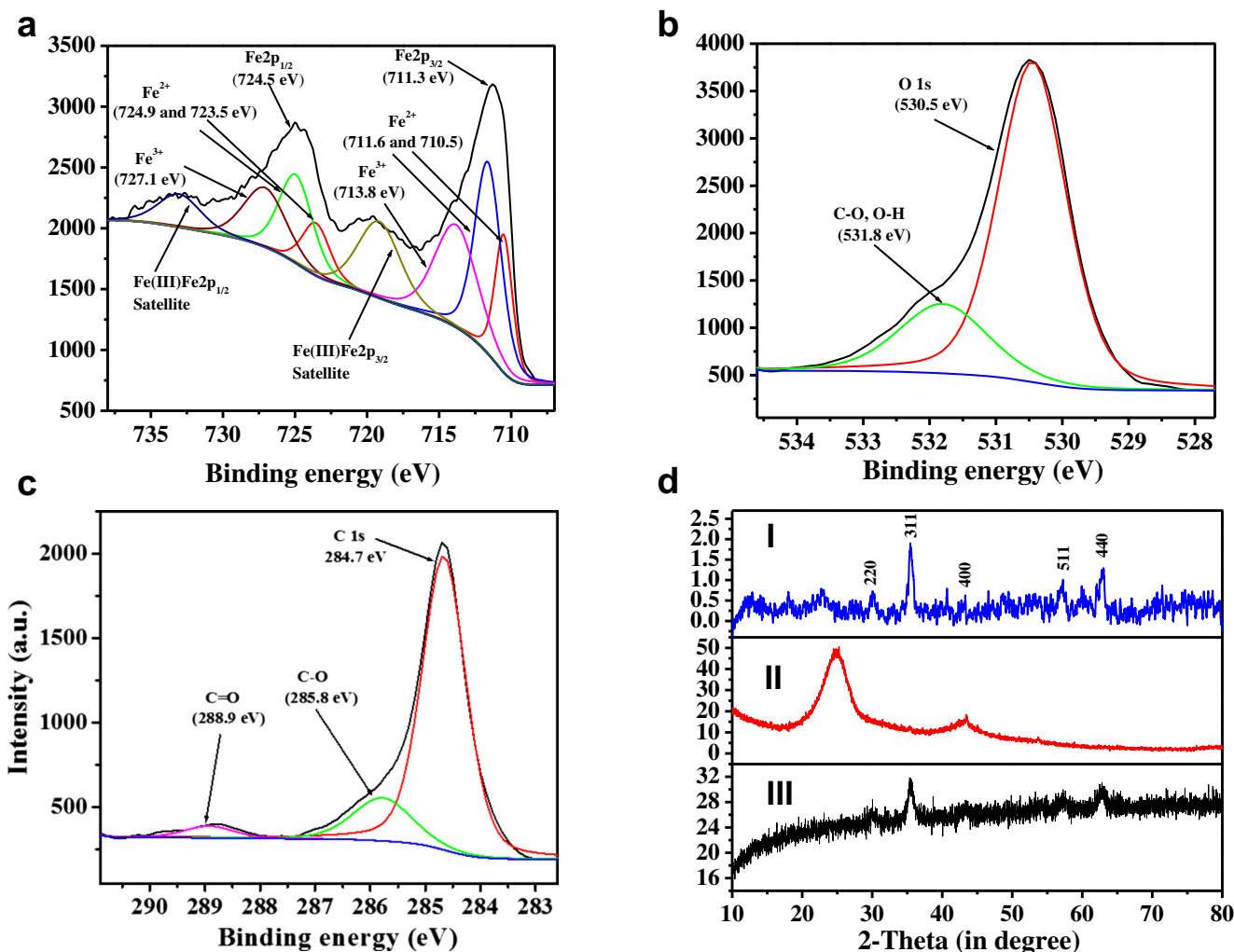

Fig. 1 (**a-c**) XPS spectra of Fe 2p, O 1s and C 1s for the CB-Fe₃O₄ nanocomposite, respectively, and (**d**) XRD patterns of (**I**) CB-Fe₃O₄ nanocomposite, (**II**) CB and (**III**) Fe₃O₄ NPs

285.8 and 288.9 eV, which were assigned to C-C, C-OH and C=O, respectively. The C-C peak is mainly attributed to the carbonaceous materials from the CB, whereas C-O and C=O is assigned to the partially dehydrated residues on the surface of the nanocomposite [19].

Figure 1d (**I-III**) show the XRD patterns of the CB-Fe_3O_4 nanocomposite, CB and Fe_3O_4 NPs. In Fig. 1d (**I**), the position and relative intensities of all the diffraction peaks obtained for the CB-Fe_3O_4 nanocomposites at $2\theta = 30.20, 35.60,$ 43.40, 57.10 and 62.90° correspond to those of the 220, 311, 400, 511 and 440 basal planes of magnetite, respectively, which confirmed the presence of the pure cubic spinel crystal structure of Fe_3O_4, as shown by Fig. 1d (**III**) [20]. However, the broad peaks characteristic of carbonaceous CB at $2\theta = 24$ and 42° [21] disappeared in the XRD pattern of the nanocomposites, as illustrated for the pure CB shown in Fig. 1d (**II**), which is due to the low concentration of CB used to prepare the nanocomposite. Therefore, the Raman spectroscopy measurements were carried out to further elucidate the formation of the CB-Fe_3O_4 magnetic nanocomposite and to characterize the structural features of the carbonaceous materials [22]. Figure 2a shows the Raman spectrum obtained for the nanocomposite; the peaks at 213, 273, 393, 483 and 595 cm^{-1} were assigned to the Fe-O and Fe-C bonds in Fe_3O_4 [23], while, on the other hand, the two peaks observed at approximately 1340 cm^{-1} and 1600 cm^{-1} in the spectrum correspond to the D and G bands of the carbonaceous materials, respectively [24]. Thus, the mixed phase structure of the individual

components confirms the formation of the CB-Fe_3O_4 magnetic nanocomposite.

The chemical interactions between the substrate and the analyte molecules are of paramount importance for stimulating selective and efficient extraction and sensitive laser desorption/ionization (LDI) detection of analytes by the substrate [25]. Depending on the nature of the analyte and the surface chemistry of the substrate, the specificity of a SELDI probe can be tuned for the adsorption of a wide range of molecules, or its affinity for a specific type of compound can be limited. Therefore, the FT-IR spectral analysis was conducted to investigate the functional groups present on the magnetic nanocomposite (Fig. 2b). The characteristic peaks at 1629 and 1427 cm^{-1} observed in the FT-IR spectrum of the magnetic nanocomposite corresponded to the C=C and C-O stretching vibrations, respectively, while the broad peak at 3432 cm^{-1} was ascribed to the stretching vibration of O-H [26]. In addition, the spectrum of the CB-Fe_3O_4 nanocomposites showed two overlapping peaks at 588 and 631 cm^{-1}, which can be attributed to the Fe-O bond stretching vibrations of Fe_3O_4 [27]. Therefore, this analysis proved that the chemical composition of the magnetic nanocomposite can stimulate different chemical interactions with the targeted analyte due to the presence of different functional groups through interactions, such as hydrogen bonding and van der Waals interactions.

The efficiency of the substrate to absorb laser irradiation and the ability of the substrate to subsequently transfer the
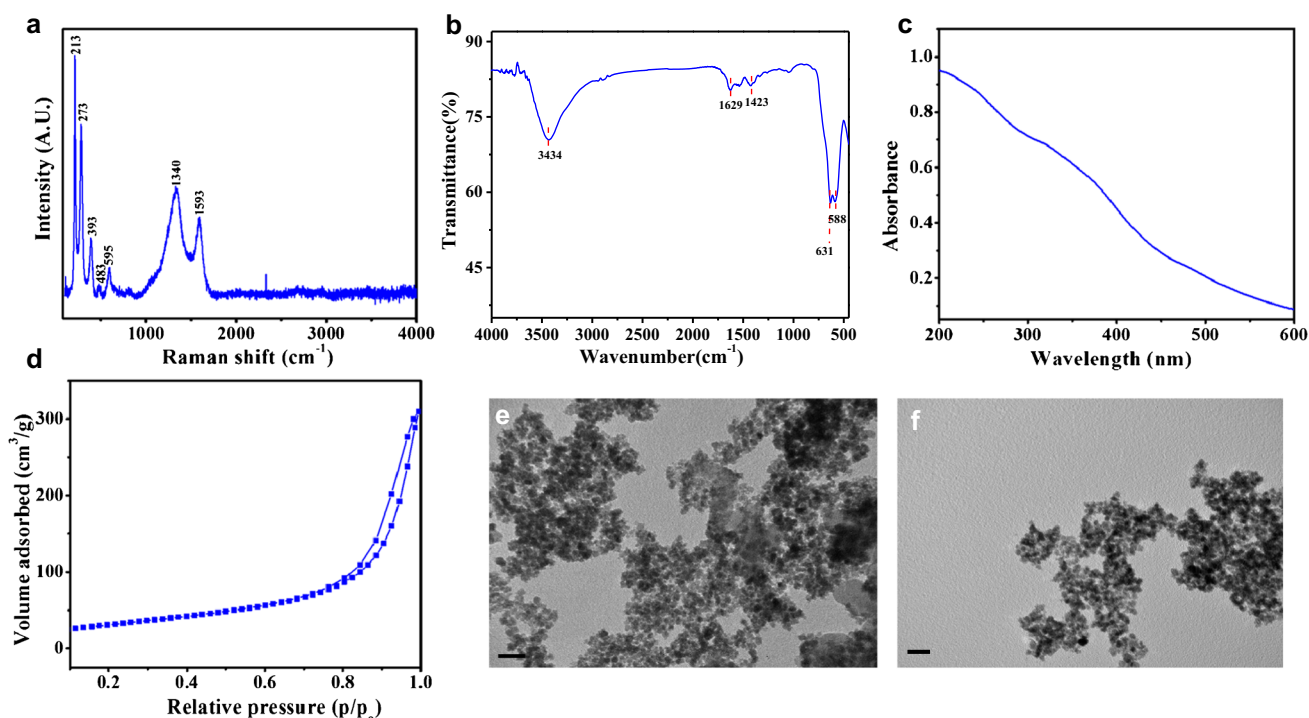

Fig. 2 (**a**) Raman spectrum; (**b**) FT-IR spectrum; (**c**) UV-Vis spectrum; (**d**) N_2 adsorption isotherm; and (**e**) and (**f**) TEM images of the synthesized CB-Fe_3O_4 nanocomposite. The scale bar is 100 nm

irradiation to the analyte(s) are vital factors in determining SELDI performance. Therefore, substrates that have substantial absorptivity in the UV-Vis region are potential candidates for SELDI technologies [28]. Therefore, the UV-Vis spectrum of the CB-Fe$_3$O$_4$ nanocomposite (Fig. 2c) was obtained to assess the absorption efficiency of the magnetic nanocomposite in the UV-Vis region. Patently, the absorption occurring from 200 to 600 nm was observed in the UV-Vis spectrum of the magnetic nanocomposite, which can be ascribed to the d orbital transitions of Fe$_3$O$_4$ [29], whereas the peak at approximately 240 nm can be assigned to the π- π* absorption of the CB. Thus, the high absorption efficiency of the magnetic nanocomposite in the UV-Vis region leads to its potential applicability in SELDI analysis.

The surface capacity of the probe plays an important role in the adsorption of the analyte, and a large surface area provides a high loading capacity of the analyte molecules, thereby improving the SELDI performance [10]. Therefore, to validate the surface properties of the magnetic nanocomposites, N$_2$ adsorption-desorption was employed, as shown in Fig. 2d. The obtained N$_2$ isotherm can be characterized as type-IV, and the hysteresis loop can be classified as H3, indicating the mesoporous nature of the nanocomposite [30]. The N$_2$ sorptometry measurements revealed that the surface area of the CB-Fe$_3$O$_4$ nanocomposite significantly increased from 60.09 to 115.10 m^2 g^{-1} with respect to the pristine CB. Additionally, both the pore volume (V$_p$) and pore diameter (D$_p$) of the magnetic nanocomposite dramatically increased from 0.0002 to 0.010 cm^3 g^{-1} and 8.32 to 16.6 nm compared to the pristine CB, respectively. Consequently, the enlarged surface area of the magnetic nanocomposite compared to the pristine CB can enhance and improve its SELDI performance.

The morphologies of the CB-Fe$_3$O$_4$ nanocomposite were analyzed using TEM, as shown in Fig. 2e-f. The TEM images of the CB-Fe$_3$O$_4$ nanocomposite showed that most of the particles were spherical in shape and approximately 30 nm in size.

Application of the SELDI probe for the analysis of spiked wine

In SELDI technologies, different properties should be considered to construct a probe with a high extraction efficiency and sensitive detection of the analyte. Of these properties, the scaffold chemistry of the substrate can promote different binding interactions with the analyte, including hydrophobic, van der Waals, hydrogen and electrostatic interactions. Furthermore, the surface capacity of the probe plays a vital role in SELDI analysis, and thus, a probe with a high surface capacity can explicitly bind to a large number of analytes;

meanwhile, the functional groups present on the surface of the probe can stimulate selective and specific binding interactions with the analyte, thereby enhancing the extraction efficiency of the probe [10].

The amount of the SELDI probe used is a pivotal factor in the analysis and represents the capacity of the probe to extract the analyte of interest in the solution. Therefore, the extraction efficiency of the magnetic nanocomposite was initially optimized using 10, 5 and 1 mg of the magnetic SELDI probe. All the nanocomposites performed well as SELDI probes and exhibited a high detection sensitivity for the analytes (note that the results are not shown). However, to avoid background signals and/or ion source contamination, which can result from the use of carbon-based materials [31], the lowest concentration of the magnetic probe (1 mg) was employed in the following experiments.

Initially, the unspiked wine was analyzed using the magnetic probe, as shown in Fig. 3. Patently, the mass spectrum was very clean and had a low background signal, and almost no fragments were obtained. Additionally, a high signal intensity was observed at 218.9 m/z, which corresponded to the potassium adduct of glucose and/or fructose, which are present in high concentrations in wine. Upon enlarging the spectrum between 100 and 219 and 215–500 m/z, more features were observed, confirming the presence of other constituents in wine (Fig. 3b and c). In Fig. 3b, peaks at 150.3, 156.7, 202.7 and 212.7 m/z can be assigned to the radical cation of tartaric acid, the sodium adduct of malic acid, the sodium adduct of glucose and/or fructose and the potassium adduct of the amino acid arginine, respectively. On the other hand, in Fig. 3c, a peak at 220.8 m/z was detected, corresponding to the potassium adduct of mannitol and/or sorbitol molecule(s).

Then, three different classes of drugs, namely, β-blockers, antidepressants and antihistamines, were spiked into wine and applied for the SELDI analysis using the magnetic nanocomposite, as shown in Table 1 and Fig. 4a-c. All the mass spectra showed pronounced signal intensities of the drugs with minimum background signals and fragmentation. Figure 4a shows the positive ion mass spectra representative of the β-blockers labetalol and metoprolol obtained using the magnetic probe. Surprisingly, both drugs were detected in their potassium forms, and labetalol and metoprolol had LODs of 1000 and 100 pg mL^{-1}, respectively. Furthermore, Fig. 4b shows peaks at 267.5, 280.4, 305.4 and 318.4 m/z, which were ascribed to [desipramine + H]$^+$, [doxepin + H]$^+$, [desipramine + K]$^+$ and [doxepin + K]$^+$, respectively, and the LOD of this class of drugs was 1.0 pg mL^{-1}. The high signal intensity of the doxepin molecule compared to the desipramine molecule can be attributed to the nature of the analyte [32], which enhanced the interaction between the substrate and analyte and
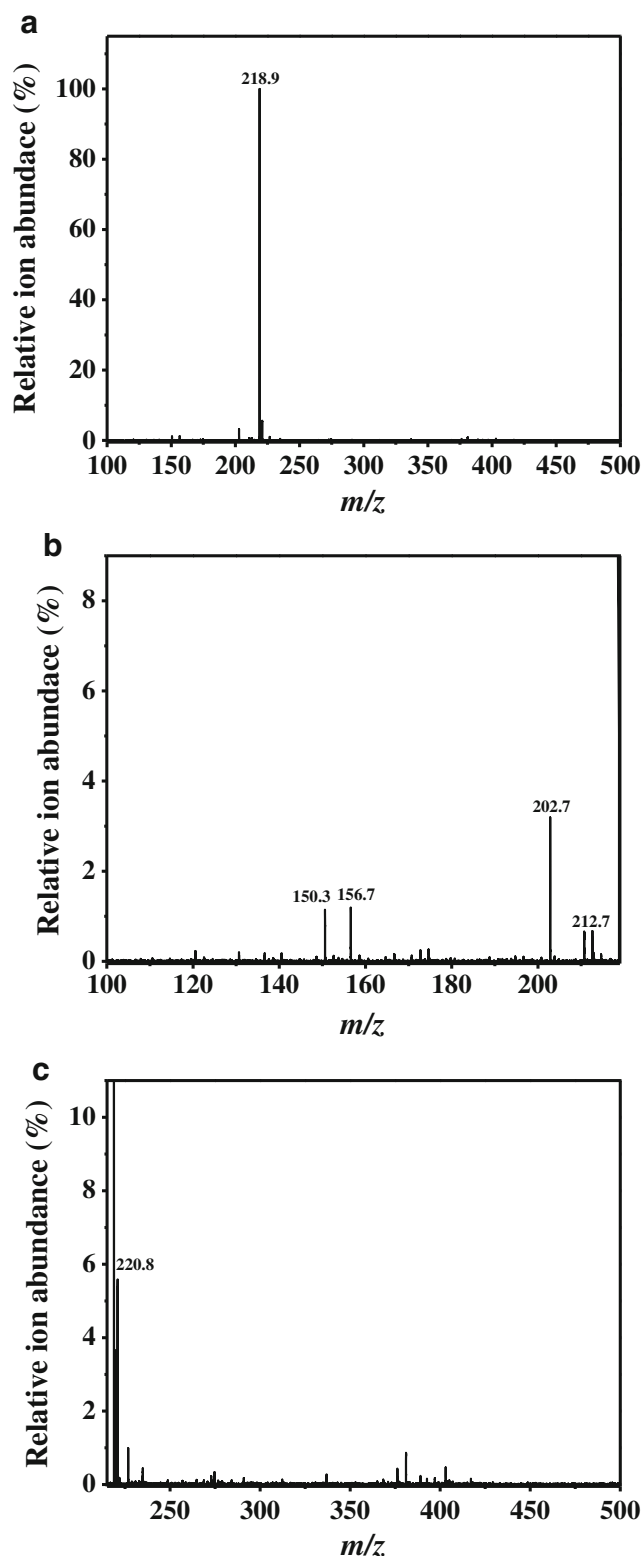
a

b

c

Fig. 3 (**a**) Analysis of the unspiked wine using the magnetic nanocomposite-based SELDI probe; (**b**) enlargement of **a** from 100 to 219 *m/z*; and (**c**) enlargement of **a** from 215 to 500 *m/z*. The spectrum was obtained in positive ionization mode using 20% laser power

Table 1 The intensity (I) and %RSD of the spiked drug analytes (1 mg mL^{-1}) using the magnetic nanocomposite SELDI probe; the results were obtained using a laser power of 20% and 500 shots, where $n = 5$–6

Analyte	m/z	Intensity	%RSD	LOD (pg mL^{-1})
β-Blockers				
Labetalol: [M + K]$^+$	367	770.0	26.5	1000
Metoprolol: [M + K]$^+$	306	898.5	24.2	100
Antidepressants				
Doxepin: [M + H]$^+$	280.4	328.3	21.7	1.0
[M + K]$^+$	318.4	110.3	15.1	1.0
Desipramine: [M + H]$^+$	267.5	40.6	27.7	1.0
[M + K]$^+$	305.4	19.4	31.1	1.0
Antihistamines				
Methapyrilene: [M + K]$^+$	300.3	186.5	21.6	10
Triprolidine: [M + K]$^+$	317.3	338.3	30.4	1000

prevented the early desorption of the analyte via thermal effects [33]. Finally, the analysis of the antihistamine showed peaks at 300.3 and 317.3 *m/z*, which corresponded to the potassium adducts of the methapyrilene and triprolidine molecules, respectively; the potassium adducts of the methapyrilene and triprolidine molecules had LODs of 10 and 1000 pg mL^{-1}, respectively (Fig. 4c). Thus, these findings proved that all the compounds were extracted and were detected with high efficiencies, which can be attributed to the strong binding affinity between the targeted analyte and the magnetic nanocomposite.

Adsorption experiment

The adsorption efficacy is a critical factor in SELDI technology, especially when high throughput and efficiency are imperative elements in the analysis. Therefore, the adsorption capacity of the magnetic SELDI probe towards three classes of drugs was explored. To assess the amount of drugs adsorbed on the magnetic nanocomposite and to eliminate the contribution of wine, the drugs were spiked into DI-water, and then, the magnetic nanocomposite was introduced into the solution. The solution mixture was vortexed for 3 min, and the remaining concentration of drugs in the solution was determined by a UV-Vis spectrometer. The AE of the investigated probe was determined using Eq. 1, and the results are shown in Table 2. The findings showed that, within 3 min, the average AE of the magnetic SELDI probe towards the ß-blockers, antidepressants and antihistamines were 35.94, 27.78 and 36.06%, respectively.
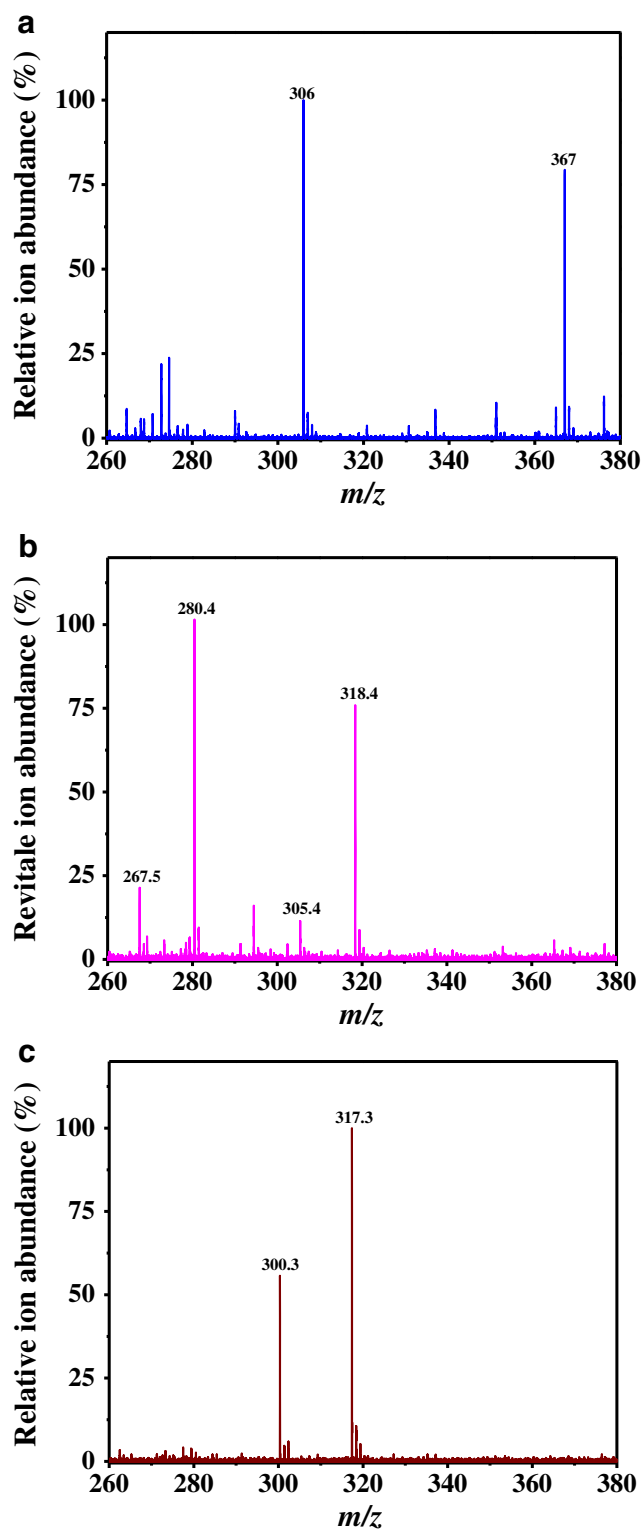
a

b

c

Fig. 4 Mass spectra of (**a**) the β-blockers (1 mg mL^{-1}): labetalol (M + K = 367 m/z) and metoprolol (M + K = 306); (**b**) the antidepressants (1 mg mL^{-1}): doxepin (M + H = 280 m/z, M + K = 318.4 m/z) and desipramine (M + H = 267.5 m/z, M + K = 305.4 m/z); and (**c**) the antihistamines (1 mg mL^{-1}): methapyrilene (M + K = 300.3 m/z) and triprolidine (M + K = 317.3 m/z). All the drugs were spiked in wine, and the spectra were obtained using the magnetic nanocomposite-based SELDI probe in positive ionization mode with 20% laser power

Table 2 Average adsorption efficiency and %RSD for the analysis of spiked drug molecules (100 μg mL^{-1}) using the magnetic nanocomposite SELDI probe, where $n = 3$

Drug	Average AE (%)	RSD (%)
ß-blockers*	35.94	3.3
Antidepressants**	27.78	8.1
Antihistamines***	36.06	9.9

*Wavelength used for the calculation is 220 nm

**Wavelength used for the calculation is 226 nm

***Wavelength used for the calculation is 247 nm

Furthermore, the effect of time on the AE of the SELDI probe for the drugs was investigated and shown in Fig. 5. The AE of the SELDI probe for the drugs drastically increased after 3 min, and then, a state of equilibrium was achieved after almost 4 min of the adsorption process. This can be attributed to the accessibility of the vacant surface sites on the magnetic SELDI probe for the immediate adsorption of the drug during the initial stage [34]. These results proved that the magnetic nanocomposite can be used as an efficient probe for SELDI analysis, enabling the simple and rapid extraction of various substances that might be present in individual's drinks.

Application of the SELDI probe for the analyses of amino acids and fatty acids

To further validate the use of the magnetic SELDI probe for the analysis of nonconjugated small molecules, extraction and detection were carried out for amino acids and fatty acids, which are examples of species involved in physiological and pathological processes. To perform the validation, a mixture of three amino acids, serine, valine and tryptophan, and two
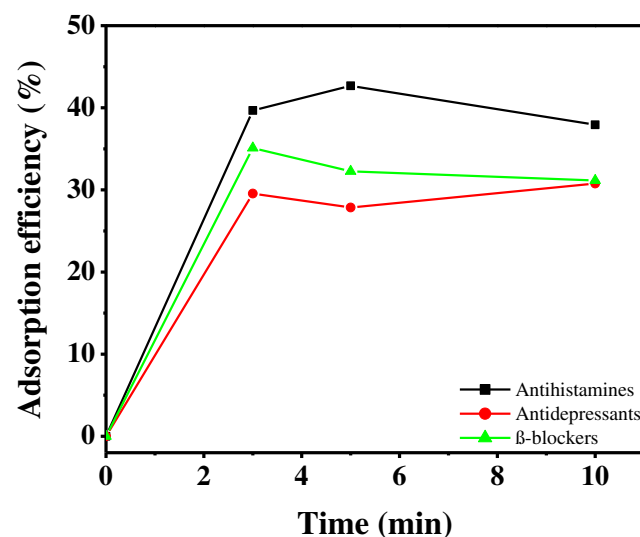

Fig. 5 The effect of time on the adsorption efficiency of different drugs (100 μg mL^{-1}) onto the magnetic SELDI probe

fatty acids, myristic acid (C14) and arachidic acid (C20), were analyzed, as shown in Fig. 6a-b. The SELDI spectrum obtained for the amino acids had low background ion interferences and showed peaks at 103.8, 115.9 and 202.9 m/z, which corresponded to the deprotonated forms of serine, valine and tryptophan, respectively (Fig. 6a). A high signal intensity was observed for the peak corresponding to the deprotonated form of serine, whereas the peak corresponding to tryptophan had a relatively low signal intensity. The labeled peak at 112.5 m/z can be assigned to $[\text{valine-2CH}_3 + \text{Cl}]^-$, resulting from the fragmentation of valine at a high laser power.

In contrast, the spectrum of the fatty acids demonstrated peaks at 226.9 and 311.1 m/z, which can be ascribed to the deprotonated forms of myristic acid (C14) and arachidic acid (C20), respectively (Fig. 6b). Importantly, the signal intensity
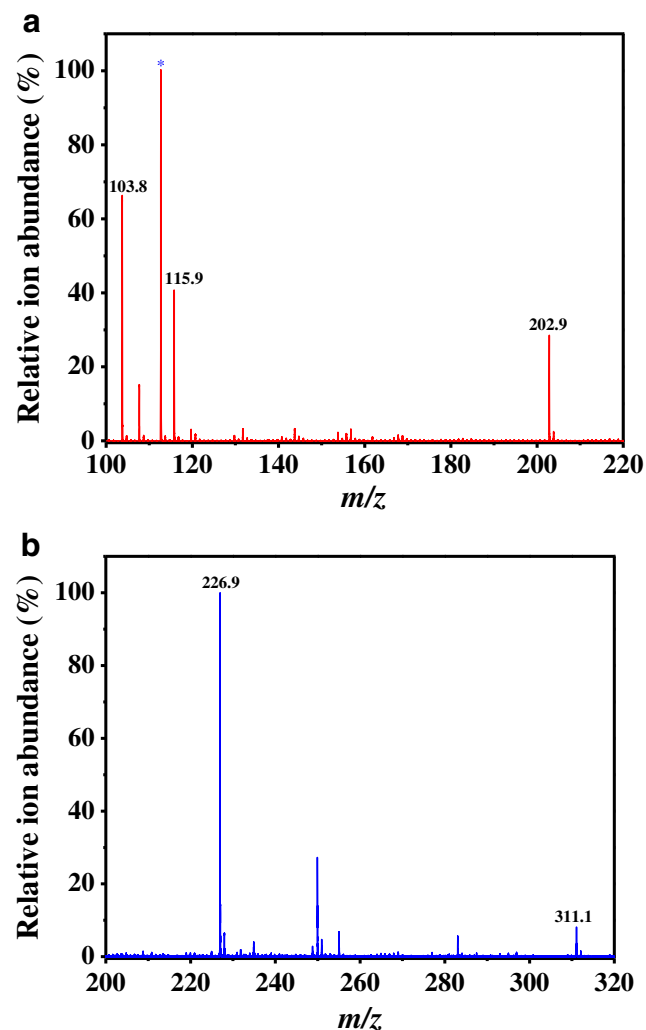
of the peak corresponding to the fatty acid with the shorter chain (C14) was more pronounced than that of its longer chain counterpart (C20). Thus, the investigated probe can be used to extract and subsequently detect both conjugated and nonconjugated analytes.

Conclusions

A novel and simple magnetic SELDI-MS probe was fabricated and characterized using various analytical instruments including XPS, XRD, Raman spectroscopy, FT-IR, UV-Vis spectroscopy, TEM and N_2 sorptometry. The findings showed the successful formation of the magnetic nanocomposite, and the magnetic nanocomposite was shown to have a high content of Fe_3O_4 and an enlarged surface area compared to carbon black (CB). The nanocomposite was applied as a platform for the rapid extraction and subsequent analysis of various drugs spiked in wine. All the drugs were detected in their potassiated forms with a satisfactory limit of detection. The adsorption capacity of the magnetic SELDI probe was examined, and this study proved that the magnetic nanocomposite enabled the successful extraction of the targeted drugs. In addition, to test the applicability of the probe, it was applied for the analysis of amino acids and fatty acids, and the findings showed that all of the analytes were successfully extracted and detected. Thus, the high efficiency of this method will advance material science and will enable the use of SELDI-MS as an effective analytical tool that can be employed for routine analysis in various laboratories. However, the selectivity of this probe is an issue that can result in the extraction of several undesired compounds in the sample matrix. This can be circumvented by functionalizing the probe with more selective functional groups to promote the binding affinity of the probe towards the analyte of interest.

Fig. 6 Mass spectra of (**a**) the amino acids (1 mg mL^{-1}): serine (M-H = 103.8 m/z), valine (M-H = 115.9 m/z) and tryptophan (M-H = 202.9 m/z) and (**b**) the fatty acids (1 mg mL^{-1}): C14 (M-H = 226.9 m/z) and C20 (M-H = 311. m/z). Both spectra were obtained using the magnetic nanocomposite-based SELDI probe in negative ionization mode at 40% laser power. The asterisk marks possible valine fragments in the spectrum

References

1. Equitz TR, Rodriguez-Cruz SE (2017) High-throughput analysis of controlled substances: combining multiple injections in a single experimental run (MISER) and liquid chromatography–mass spectrometry (LC-MS). Forensic Chem 5:8–15

2. Lim AY, Ma J, Boey YCF (2012) Development of nanomaterials for SALDI-MS analysis in forensics. Adv Mater 24(30):4211–4216

3. Kong X et al (2005) High-affinity capture of proteins by diamond nanoparticles for mass spectrometric analysis. Anal Chem 77(1): 259–265

4. Huang X, Liu Q, Jiang G (2019) Tuning the performance of graphene as a dual-ion-mode MALDI matrix by chemical functionalization and sample incubation. Talanta 199:532–540

5. Grim DM, Siegel J, Allison J (2002) Evaluation of laser desorption mass spectrometry and UV accelerated aging of dyes on paper as tools for the evaluation of a questioned document. J Forensic Sci 47(6):1265–1273

6. Amin MO, Madkour M, Al-Hetlani E (2018) Metal oxide nanoparticles for latent fingerprint visualization and analysis of small drug molecules using surface-assisted laser desorption/ionization mass spectrometry. Anal Bioanal Chem:1–13

7. Al-Hetlani E et al (2018) CeO2-CB nanocomposite as a novel SALDI substrate for enhancing the detection sensitivity of pharmaceutical drug molecules in beverage samples. Talanta 185:439–445

8. Abdelmaksoud HH, Guinan TM, Voelcker NH (2017) Fabrication of nanostructured mesoporous germanium for application in laser desorption ionization mass spectrometry. ACS Appl Mater Interfaces 9(6):5092–5099

9. Hutchens TW, Yip TT (1993) New desorption strategies for the mass spectrometric analysis of macromolecules. Rapid Commun Mass Spectrom 7(7):576–580

10. Tang N, Tornatore P, Weinberger SR (2004) Current developments in SELDI affinity technology. Mass Spectrom Rev 23(1):34–44

11. Zhang Y, Wang X, Shan W, Wu B, Fan H, Yu X, Tang Y, Yang P (2005) Enrichment of low-abundance peptides and proteins on zeolite nanocrystals for direct MALDI-TOF MS analysis. Angew Chem 117(4):621–623

12. Tian R, Zhang H, Ye M, Jiang X, Hu L, Li X, Bao X, Zou H (2007) Selective extraction of peptides from human plasma by highly ordered mesoporous silica particles for peptidome analysis. Angew Chem 119(6):980–983

13. Chen H, Deng C, Li Y, Dai Y, Yang P, Zhang X (2009) A facile synthesis approach to C8-functionalized magnetic carbonaceous polysaccharide microspheres for the highly efficient and rapid enrichment of peptides and direct MALDI-TOF-MS analysis. Adv Mater 21(21):2200–2205

14. Wulfkuhle JD, Liotta LA, Petricoin EF (2003) Early detection: proteomic applications for the early detection of cancer. Nat Rev Cancer 3(4):267

15. Zhukov TA, Johanson RA, Cantor AB, Clark RA, Tockman MS (2003) Discovery of distinct protein profiles specific for lung tumors and pre-malignant lung lesions by SELDI mass spectrometry. Lung Cancer 40(3):267–279

16. Zhang W, Kong C, Lu G (2015) Super-paramagnetic nano-Fe3O4/graphene for visible-light-driven hydrogen evolution. Chem Commun 51(50):10158–10161

17. Dedryvere R et al (2008) X-ray photoelectron spectroscopy investigations of carbon-coated Li x FePO4 materials. Chem Mater 20(22):7164–7170

18. Li G, Li R, Zhou W (2017) A wire-shaped supercapacitor in micrometer size based on Fe 3 O 4 Nanosheet arrays on Fe wire. Nano-Micro Lett 9(4):46

19. Bhuvaneswari S, Pratheeksha PM, Anandan S, Rangappa D, Gopalan R, Rao TN (2014) Efficient reduced graphene oxide grafted porous Fe3O4 composite as a high performance anode material for Li-ion batteries. Phys Chem Chem Phys 16(11):5284–5294

20. Cazetta AL, Pezoti O, Bedin KC, Silva TL, Paesano Junior A, Asefa T, Almeida VC (2016) Magnetic activated carbon derived from biomass waste by concurrent synthesis: efficient adsorbent for toxic dyes. ACS Sustain Chem Eng 4(3):1058–1068

21. Ungar T et al (2002) Microstructure of carbon blacks determined by X-ray diffraction profile analysis. Carbon 40(6):929–937

22. Sadezky A, Muckenhuber H, Grothe H, Niessner R, Pöschl U (2005) Raman microspectroscopy of soot and related carbonaceous materials: spectral analysis and structural information. Carbon 43(8):1731–1742

23. Hu X, Liu B, Deng Y, Chen H, Luo S, Sun C, Yang P, Yang S (2011) Adsorption and heterogeneous Fenton degradation of 17α-methyltestosterone on nano Fe3O4/MWCNTs in aqueous solution. Appl Catal B Environ 107(3–4):274–283

24. Shu J, Cheng S, Xia H, Zhang L, Peng J, Li C, Zhang S (2017) Copper loaded on activated carbon as an efficient adsorbent for removal of methylene blue. RSC Adv 7(24):14395–14405

25. Yagnik GB, Hansen RL, Korte AR, Reichert MD, Vela J, Lee YJ (2016) Large scale nanoparticle screening for small molecule analysis in laser desorption ionization mass spectrometry. Anal Chem 88(18):8926–8930

26. Mohan AN, Manoj B (2012) Synthesis and characterization of carbon nanospheres from hydrocarbon soot. Int J Electrochem Sci 7: 9537–9549

27. Amiri A, Baghayeri M, Sedighi M (2018) Magnetic solid-phase extraction of polycyclic aromatic hydrocarbons using a graphene oxide/Fe3O4@ polystyrene nanocomposite. Microchim Acta 185(8):393

28. Chiang C-K, Chen W-T, Chang H-T (2011) Nanoparticle-based mass spectrometry for the analysis of biomolecules. Chem Soc Rev 40(3):1269–1281

29. Panwar V, Kumar P, Bansal A, Ray SS, Jain SL (2015) PEGylated magnetic nanoparticles (PEG@ Fe3O4) as cost effective alternative for oxidative cyanation of tertiary amines via CH activation. Appl Catal A Gen 498:25–31

30. Thommes, M., et al. (2015) Physisorption of gases, with special reference to the evaluation of surface area and pore size distribution (IUPAC technical report), In: Pure and applied chemistry. p. 1051

31. Tang H-W, Ng KM, Lu W, Che CM (2009) Ion desorption efficiency and internal energy transfer in carbon-based surface-assisted laser desorption/ionization mass spectrometry: desorption mechanism (s) and the design of SALDI substrates. Anal Chem 81(12): 4720–4729

32. Amin MO, Al-Hetlani E (2019) Tailoring the surface chemistry of SiO2-based monoliths to enhance the selectivity of SALDI-MS analysis of small molecules. Talanta 200:458–467

33. Lim AY, Gu F, Ma Z, Ma J, Rowell F (2011) Doped amorphous silica nanoparticles as enhancing agents for surface-assisted time-of-flight mass spectrometry. Analyst 136(13):2775–2785

34. Ai L, Zhang C, Liao F, Wang Y, Li M, Meng L, Jiang J (2011) Removal of methylene blue from aqueous solution with magnetite loaded multi-wall carbon nanotube: kinetic, isotherm and mechanism analysis. J Hazard Mater 198:282–290